

# Effect of a first-order ridge on grain boundary motion in Zn

V.G. Sursaeva<sup>b</sup>, G. Gottstein<sup>a,\*</sup>, L.S. Shvindlerman<sup>a,b</sup>

<sup>a</sup> *Institut für Metallkunde und Metallphysik, RWTH Aachen University, Germany*

<sup>b</sup> *Institute of Solid State Physics, Russian Academy of Sciences, Chernogolovka, Moscow District 142432, Russia*

Received 17 June 2010; received in revised form 28 September 2010; accepted 29 September 2010

Available online 26 October 2010

## Abstract

The migration of a grain boundary system with ridges of the first order is studied. A theory of steady-state motion of a grain boundary half-loop with facets and ridges is elaborated. The shape and properties of a moving grain boundary which contains additional structural elements (curved segments, facets and ridges of the first order) are addressed. The major kinetic parameters (mobility and its activation enthalpy) of a “rough-to-rough” grain boundary ridge of the first order were measured. It is shown that the steady-state motion of a boundary half-loop with facets and ridges complies with the principle of maximum rate of free energy dissipation.

© 2010 Acta Materialia Inc. Published by Elsevier Ltd. All rights reserved.

**Keywords:** Grain boundary motion; Grain boundary ridge; Facets; Irreversible thermodynamics

## 1. Introduction

Traditionally, grain growth in polycrystals is attributed solely to the motion of grain boundaries. With growing interest in fine-grained and even nanocrystalline materials, the need has arisen to consider the role of other structural grain boundary elements: facets, triple and quadruple junctions [1–15].

In particular, it has been shown that the kinetics of grain boundary triple and quadruple junctions may be different from the kinetics of the adjoining grain boundaries. This affects the kinetics of microstructure evolution during grain growth, especially in fine-grained materials [1–6,13–15].

It has long been known that the surface of minerals is often composed of planar faces, which are referred to as facets. They are due to the crystalline nature of the materials and reflect the anisotropy of the surface energy. However, facets are not only observed on external crystal surfaces, but can also occur on internal interfaces, like grain boundaries, and appear as straight grain boundary segments in an optical micrograph. Prominent examples are coherent

twin boundaries in low stacking fault energy materials [16]. Facets on grain boundaries are a manifestation of the anisotropy of the grain boundary surface energy; in particular, grain boundary faceting appears at grain boundaries with special misorientation, so-called low  $\Sigma$  coincidence boundaries. In spite of numerous studies dedicated to grain boundary faceting (see e.g. [7–9,17–19]), their behavior is still very poorly understood, especially how they affect grain growth. This is because the influence of a facet on grain boundary migration depends on both the thermodynamic and kinetic characteristics of the facets [1]. Only recently quantitative methods were put forward to tackle this problem [10–12]. The migration of incoherent twin grain boundaries with facets was studied by Straumal et al. [20]. It was demonstrated that the rather complicated kinetics of grain boundary motion, in particular the strong non-Arrhenius temperature dependence, could be explained by considering the motion of two competitive facets. Rabkin considered the influence of grain boundary faceting on grain growth and the motion of a two-dimensional grain boundary half-loop [10].

Studies of the influence of facets on the migration of a high angle grain boundary during steady-state motion were recently reported [11,12]. For the first time the mobility of the facets of a high angle boundary was measured in a reproducible physical experiment. A surprising result from

\* Corresponding author.

E-mail address: [Gottstein@imm.rwth-aachen.de](mailto:Gottstein@imm.rwth-aachen.de) (G. Gottstein).

Refs. [11,12] was the high facet mobility with very low activation enthalpy.

Moreover, the observed increase in the facet length with increasing facet mobility (respectively decrease in the mobility of an attached curved boundary) seems counterintuitive, since it is a frequent observation that faceted boundaries move with low mobility.

It was shown [12] that the observed behavior of steady-state motion of a faceted boundary half-loop can be explained on the basis of the Onsager principle of irreversible thermodynamics, i.e. the observed dynamic facet length corresponds to a maximum dissipation rate of free energy.

However, besides the grain boundary itself, and boundary triple and quadruple junctions and facets, there is another kind of grain boundary structure element: the grain boundary ridge. As early as 1951, Herring pointed out that an equilibrium shape of a crystal can contain edges and corners even though there are no flat facets [21]. The concept of grain boundary ridges was developed by Cahn and Hoffmann in 1974 [22]. They proved that two curved (rough) surfaces may intersect along a line where the boundary plane changes discontinuously. This line is called a first-order “rough-to-rough” ridge. Besides the first-order ridge, there also exists a ridge of the second order (without discontinuity), which has also been analyzed, mainly on the free surfaces of crystals [23–25]. A classification of various grain boundary ridges is given in Ref. [26].

As much as grain boundary motion can be affected by triple junctions, a first-order ridge may also tangibly impact the kinetics of grain boundary motion and grain growth. The major goal of the current study was to explore the steady-state motion of high angle grain boundaries with the facets, the formation of the first-order ridge and the quantitative determination of both the kinetic properties of the grain boundary system with the ridge and of the ridge itself.

## 2. Experimental

The experimental technique of the crystal manufacture was described comprehensively in Refs. [1,21]. Flat bicrystals from 99.999 wt.% Zn with a grain boundary half-loop (Fig. 1) were grown. The misorientation angle of a  $[10\bar{1}0]$  tilt grain boundary half-loop is  $30^\circ$ . The reciprocal density of

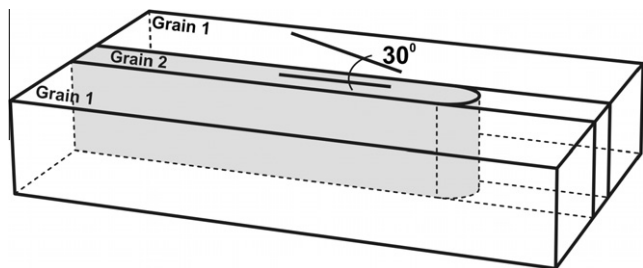


Fig. 1. Scheme of the Zn bicrystal containing the  $[10\bar{1}0]$  tilt grain boundaries with misorientation angles of  $30^\circ$ . The lines denote the orientation of basal plane (0001) in both grains [11].

coincidence sites for the studied  $30^\circ [10\bar{1}0]$  tilt grain boundary is  $\Sigma = 17$ . Both the flat and curved grain boundary segments were oriented perpendicular to the surface of the sample. The motion of the boundary and its shape were observed and recorded in situ on the hot stage of an optical microscope in the temperature range 553–683 K using polarized light. The temperature was stable within  $\pm 0.5$  K during the measurement, and the temperature was increased for consecutive isothermal anneals by 5 or 10 K. Each isothermal anneal took 120 or 180 s; the temperature of the hot stage and the sample stabilized in a few seconds. The annealing was carried out in a protective atmosphere (pure nitrogen); samples were also protected from oxidation by a pure nitrogen atmosphere. The grain boundary shape was imaged in the course of the experiment by a video camera connected to the microscope and recorded on a VCR.

## 3. Results

The behavior of the grain boundary system in the temperature range 553–683 K was studied. At temperatures higher than 673 K the moving grain boundary half-loop comprised only continuously curved segments (Fig. 2).

Facet formation on a moving half-loop was observed during cooling (Fig. 3) [11].

The peculiarities of grain boundary half-loop motion were reported in Ref. [11]. In particular, the steady-state character of the half-loop motion was confirmed: the rate of the half-loop migration, after a short time, when the temperature of the sample was established, was found to remain constant for both faceted and non-faceted grain boundaries. The length of the facet was controlled by the temperature of the experiment [11]. The lowest temperature of grain boundary half-loop migration studied in Ref. [11] was 633 K. In accordance with the concepts which were outlined in Ref. [11], the length of the facet increased with decreasing temperature. However, as observed in the current study, a further decrease in the temperature led to a disappearance of the facet and, surprisingly, to the forma-



Fig. 2. Smooth curved grain boundary half-loop [11].

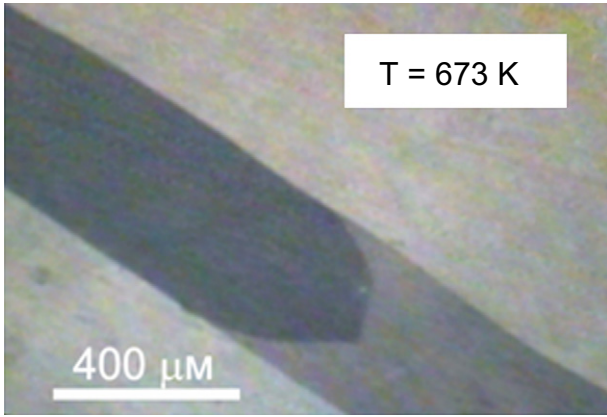


Fig. 3. Video frame of a moving grain boundary half-loop with facets.

tion of a new structural element – a grain boundary “rough-to-rough” ridge of the first order (Figs. 4 and 5).

To prove the formation of a true ridge, we used the following line of arguments.

- (a) At a high temperature the moving grain boundary half-loop was composed of smoothly curved segments only. A reduction in the temperature caused grain boundary faceting. A further fall in the temperature led to the disappearance of the facets and the formation of a “rough-to-rough” ridge. It is stressed that all discussed boundary transitions between the observed configurations were reversible.
- (b) The motion of the first-order ridge was observed in a temperature range where the triple junction motion in Zn was never found.
- (c) The ridge formation essentially changed the character of motion of the grain boundary system: instead of nearly athermal motion, which was observed for the moving faceted half-loop, the half-loop with ridge demonstrated thermally activated motion with a rather large activation enthalpy (~2.4 eV).
- (d) Orientation measurements by electron backscatter diffraction and metallographic observations did not reveal any low angle grain boundary at the ridge.



Fig. 4. Grain boundary with the “rough-to-rough” ridge of first-order at the half-loop ( $T = 345\text{ °C}$ ).

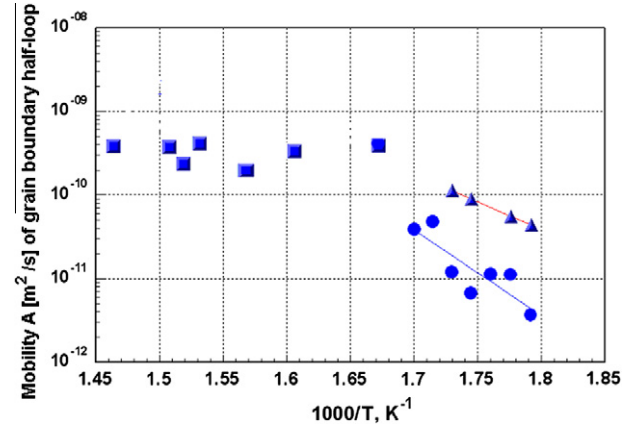


Fig. 5. Mobility  $A$  of the grain boundary half-loop ( $A = v \cdot a(\text{m}^2/\text{s})$ ) with a facet (solid squares) and with a ridge (solid circles and triangles).

- (e) Finally, the microstructure of studied bicrystals in the region of the ridge was analyzed by X-ray topography (using the Schultz technique [27,28]; the smallest misorientation between next neighbor grains that can be detected by this technique is 1–3′). The missing evidence of a misorientation at the ridge proved that the observed boundary configuration was not the consequence of a low angle boundary (at least with the misorientation larger than ~3′) attached to the tip of the ridge.

#### 4. Discussion

##### 4.1. Theory of motion of a faceted grain boundary with a ridge of the first order

Let us consider the steady-state motion of a grain boundary half-loop with a facet and a ridge of the first order (Fig. 6). The geometry resembles a faceted boundary as considered in Ref. [11] for the steady-state motion of a grain boundary half-loop with a facet.

However, as will be shown below, the existence of a ridge changes the situation substantially.

The equation of motion and the boundary conditions which define the steady-state shape and the velocity  $V$  of a partially faceted boundary read (Fig. 6)

$$y'' = -\frac{V}{\gamma_b m_b} y'(1 + y'^2)$$

$$(a) \quad y'(l \cos \theta) = \tan(\theta - \varphi)$$

$$(b) \quad y(\infty) = a/2$$

$$(c) \quad y(l \cos \theta) = l \sin \theta;$$

(1)

The shape of the moving curved segment of the half-loop without facet is described by a solution of Eq. (1) [11]; with the boundary conditions

$$(a) \quad y(0) = 0$$

$$(b) \quad y(\infty) = \frac{a}{2}$$

$$(c) \quad y'(0) = \infty$$

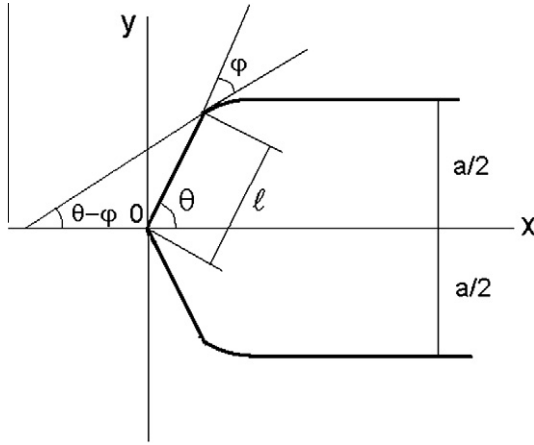


Fig. 6. Geometry of a grain boundary half-loop with a facet.

$$y(x) = \frac{a}{2} \arccos \left[ \exp \left( -\frac{2\theta}{a} x + \ln(\sin \theta) \right) \right] - \frac{a}{2\theta} \left( \frac{\pi}{2} - \theta \right);$$

$$V = 2 \frac{\theta m_b \gamma_b}{a} \quad (2)$$

Here,  $m_b$ ,  $\gamma_b$  are grain boundary mobility and surface tension, respectively.

Since the facet is flat with inclination  $\theta$  (Fig. 6), the shape of the curved part of the moving half-loop with a facet is given by the equation

$$y = \frac{a}{2} - \frac{m_b \gamma_b}{V} \frac{\pi}{2} + \frac{m_b \gamma_b}{V} \times \arccos \left[ \sin(\theta - \varphi) \exp \left( \frac{V}{m_b \gamma_b} (l \cos \theta - x) \right) \right] \quad (3)$$

To determine the velocity of the moving half-loop, we draw on boundary condition 1(c)  $y(l \cos \theta) = l \sin \theta$ , which renders

$$V = \frac{m_b \gamma_b (\theta - \varphi)}{\frac{a}{2} - l \sin \theta} \quad (4)$$

Since, for a steady-state motion, the faceted and curved segments of the half-loop and the ridge have to move with the same velocity:

$$(1) V_b = V_f$$

$$(2) V_b = V_r \quad (5)$$

$$(3) V_f = V_r$$

where  $V_b$ ,  $V_f$ ,  $V_r$  are the velocities of the curved grain boundary, of the facet and the ridge, respectively.

As shown in Ref. [11], the facet velocity can be expressed as (Fig. 6)

$$V_f = \frac{m_f \gamma_b \sin \varphi \sin \theta}{l} \quad (6)$$

where  $m_f$  is the mobility of the facet.

On the other hand,

$$V_r = 2m_r \gamma_b \cos \theta \cos \varphi \quad (7)$$

where  $m_r$  is the mobility of the ridge.

Then from Eqs. (1) and (5) we arrive at

$$l = \frac{\frac{a}{2}}{\sin \theta + \frac{m_b(\theta - \varphi)}{m_f \sin \varphi \sin \theta}} \quad (8)$$

while from Eqs. (2) and (5) we obtain

$$l = \frac{a}{2 \sin \theta} - \frac{m_b(\theta - \varphi)}{2m_r \cos \theta \sin \theta \cos \varphi} \quad (9)$$

It can be seen that Eqs. (8) and (9) comply with expectations for the limiting cases. If the mobility of the grain boundary  $m_b$  is large or the mobility of the facet  $m_f$  or the ridge  $m_r$  is small, the length of the facet tends to zero. For a facet with large mobility or for the ridge with large mobility the length approaches the maximal value  $l = \frac{a}{2 \sin \theta}$ .

Eqs. (8) and (9) allow us to derive the mobility of the facet and of the ridge and their temperature dependence from the experimentally measured values of the facet length.

The temperature dependence of the measured facet length gives the possibility of extracting the normalized facet mobility ( $m_f/m_b$ ) [11]. A reduction in the facet length with rising temperature is mainly caused by a decrease in the ratio  $m_f/m_b$ . Eqs. (8) and (9) also yield the value of the facet or ridge mobility if the grain boundary mobility is known from an independent experiment. Such a dependency for the reduced facet mobility was derived in Ref. [11] using the data of grain boundary mobility measured in Refs. [29,30].

It should be stressed that the transition “faceted grain boundary–smoothly curved (rough) boundary” proceeds through the formation of the new ridge of first-order. Instead of the “facet-to-facet” or “facet-to-rough” ridge, the system forms a “rough-to-rough” ridge.

Unfortunately, it was not possible to fix the change of the facet length during such a transition at low temperatures. That is why we attempt to estimate the mobility of the “facet-to-facet” ridge at the point where the length of the facet is equal to zero (Fig. 5,  $T = 345^\circ\text{C}$ ). From Eq. (9) we arrive at:

$$\frac{m_r a}{m_b} = \frac{\theta - \varphi}{\cos \theta \cdot \cos \varphi} \quad (10)$$

Expression (10) represents the dimensionless criterion  $A_r$ , which defines the drag effect of a ridge on the motion of the grain boundary system [1];  $A_r \approx 0.4$  under the conditions of our experiment. It indicates that the motion of the grain boundary system at this temperature was controlled by ridge kinetics. Eq. (10) makes it possible to estimate the value of the ridge mobility  $m_r$ , since the grain boundary mobility  $m_b$  is known from the independent experiment [1,29,30]:  $m_r = 5 \times 10^{-4} \text{ m}^3 \text{ J}^{-1} \text{ s}^{-1}$ .

At a temperature lower than  $345^\circ\text{C}$  the grain boundary half-loop comprises two curved boundary segments with a “rough-to-rough” ridge of the first order (Fig. 7).

Let us consider the steady-state motion of a moving half-loop with a ridge of the first order. The shape and velocity of the curved boundary are given in Eqs. (1) and

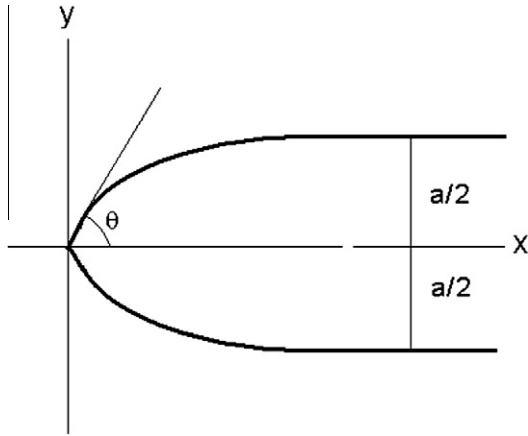


Fig. 7. Geometry of a grain boundary half-loop with a “rough-to-rough” ridge of the first order.

(2). On the other hand, the velocity of the ridge migration can be described as:

$$V_r = m_r P_r \quad (11)$$

where  $m_r$  is the mobility of the ridge and  $P_r$  is the driving force for ridge motion.

From Fig. 7 it can be seen that

$$P_r = 2\gamma_b \cos \theta \quad (12)$$

Since, for a steady-state motion, the ridge and curved segments of the half-loop have to move with the same velocity, the migration rate of the grain boundary half-loop with a ridge is also controlled by the ridge motion:

$$V = V_r \quad (13)$$

From Eqs. (2), (11), and (12) we arrive at:

$$m_r = \frac{m_b \theta}{a \cos \theta} \quad (14)$$

Apparently, relation (14) associates the angle  $\theta$  with the value of the dimensionless parameter  $A_r$

$$A_r = \frac{m_r a}{m_b} = \frac{\theta}{\cos \theta} \quad (15)$$

which characterizes the inhibiting influence of the ridge on grain boundary motion. (Compare with the parameter  $\Lambda$  for the grain boundary system with a triple junction [1].)

It can be seen that Eq. (15) matches the expectations for the limiting cases. A grain boundary ridge with large mobility  $m_r$  does not drag the motion of the grain boundary system, the angle  $\theta$  tends to  $\pi/2$  and the configuration transforms to the well-known grain boundary half-loop, where the velocity of the half-loop is determined by the grain boundary mobility. For a low-mobility ridge the angle  $\theta$  tends to zero.

#### 4.2. Determination of ridge mobility

Relation (15) makes it possible to determine the mobility of a grain boundary ridge if the grain boundary mobility  $m_b$  is measured in an independent experiment. Fig. 8 demonstrates the experimentally measured temperature dependence

of the angle between the tangents to curved boundaries at the tip of the first-order ridge. On the basis of independently measured values of grain boundary mobility  $m_b$  and data from Fig. 8, the mobility of the ridge can be defined. In the case when the migration of the half-loop is controlled by the motion of the ridge, the kinetic parameters of the migration should be determined by the parameters of the ridge. The principal argument in favour of such a behavior is the parameter  $A_r$ . As was shown in Ref. [1], the rather small value of the parameter  $\Lambda$  indicates that the ridge drags and at the same time controls the migration of the half-loop. In our case, the parameter  $A_r \approx 1.5 - 1.8$  in the measured temperature range (280–350 °C). According to Fig. 9 (see below), where  $A_r(\theta)$  is presented it follows immediately that the migration of our boundary system is determined by ridge motion since  $A_r = 1.5 - 1.8$  indicates ridge-controlled kinetics.

In Fig. 5 the mobility of the half-loop, which is defined as the velocity of the half-loop divided on the driving force (essentially the half-loop width), is marked by solid circles while the mobility of the ridge, defined as described above, is marked by solid triangles. The activation enthalpy of migration, which is determined from the half-loop motion as a whole and the ridge migration, is equal to 2.4 and 1.1 eV, respectively. The angle  $\theta$  is relatively small for low temperatures (285–290 °C) and for the highest temperature (315 °C) studied (Fig. 8). This is why the ridge mobility, as compared to the motion of the half-loop as a whole, should increase at high temperatures and decrease at low temperatures, in accordance with Eq. (14). The strong reduction in the major kinetic parameter, the enthalpy of activation, which derives from both the change of the angle  $\theta$  with temperature and the dependency  $m_r(\theta)$ , points to the fact that the migration of our grain boundary system is governed by the “rough-to-rough” ridge of first-order.

#### 4.3. Ridge motion and irreversible thermodynamics

As shown in Ref. [1], the velocity of the grain boundary half-loop can be represented as:

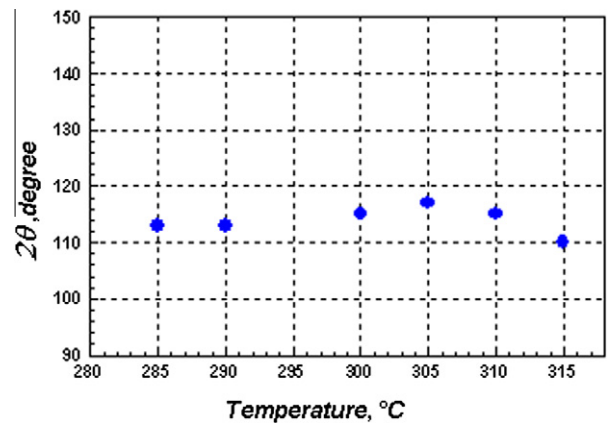


Fig. 8. Temperature dependence of the angle  $2\theta$  at the tip of the “rough-to-rough” ridge of the first order.

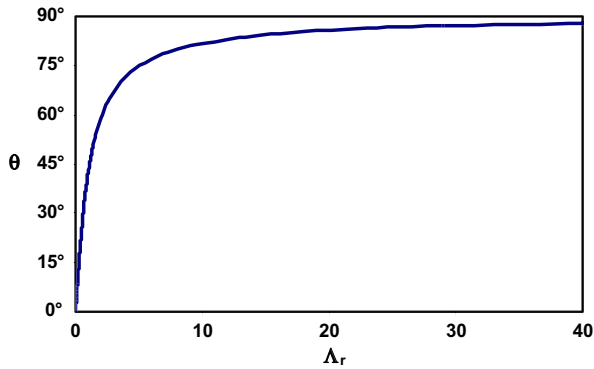


Fig. 9. Vertex angle  $\theta$  as a function of  $\Lambda_r$ .

$$V = \frac{2\gamma_b}{a} \int_0^1 \frac{m_b(\zeta V) d\zeta}{\sqrt{1-\zeta^2}} \equiv \frac{2\gamma_b}{a} M(V) \quad (16)$$

where  $\frac{2\gamma_b}{a}$  is the average driving force acting on the half-loop,  $V$  is the velocity of the half-loop as a whole and  $M(V)$  is the average mobility of the half-loop. The values of  $V$  which represent the solutions of Eq. (10) comply with the extremum of the function

$$\Psi(V) = \left[ 2\gamma_b V - a \int_0^V \frac{V dV}{M(V)} \right] \quad (17)$$

Only maxima of this function correspond to stable steady-state motion [1]. For a linear dependence of the velocity on the driving force ( $M(V) = \text{const.}$ ) the extremum of the function  $\Psi(V)$  is equivalent to the maximum rate of reduction in free energy of the system (dissipation rate), which in turn is related to the Onsager principle of irreversible thermodynamics. In other words, the system tries to reduce the free energy as quickly as possible, i.e. with the maximum possible rate. For the steady-state motion of a grain boundary half-loop with a first-order “rough-to-rough” ridge, the average mobility of  $M(V)$  can be defined in two ways: either by the ridge motion or by the motion of the curved boundary. In the first case – where the half-loop motion is controlled by the ridge motion – the average mobility can be expressed as:

$$M_f(V) = \frac{V}{2\gamma_b/a} = m_r a \cos \theta \cos \varphi \quad (18)$$

When the half-loop migration rate is determined by the motion of the curved grain boundary, the average mobility is:

$$M_b(V) = \frac{m_b(\theta - \varphi)a}{2\left(\frac{a}{2} - l \sin \theta\right)} \quad (19)$$

A maximum rate of free energy reduction in the system is obtained for a constant average mobility:

$$M_f(V) = M_b(V) \quad (20)$$

Obviously condition (20) is satisfied by relation (9). In essence, the facet changes its length in the course of motion in order to permit the system to reduce its free energy at

the highest rate. It is evident that, for the half-loop configurations presented in Fig. 7, condition (20) is satisfied by relation (9).

In other words, the observed dynamic facet length in the system with the ridge complies with the maximum dissipation rate of free energy of the system.

## 5. Conclusions

1. The steady-state migration of a special  $30^\circ [10\bar{1}0]$  tilt grain boundary half-loop with facets and with ridges of the first order was studied.
2. A theory of steady-state motion of a grain boundary half-loop with facets and ridges is presented.
3. For the first time, the mobility and the activation enthalpy of migration of a “rough-to-rough” grain boundary ridge of the first order have been measured.
4. It was shown that the peculiarities of the steady-state motion of the half-loop studies can be considered in the framework of the principle of a maximum rate of free energy dissipation.

## Acknowledgements

We appreciate the financial support of the cooperation through the DFG Grant RUS113/846/0-2(R) and the Russian Foundation of Fundamental Research (Grant DFG-RRFI 09-02-91339). The assistance of Dr. Irina Smirnova with the X-ray topography measurements is gratefully acknowledged.

## References

- [1] Gottstein G, Shvindlerman LS. Grain boundary migration in metals: thermodynamics, kinetics, applications. 2nd ed. Boca Raton (FL): CRC Press; 2010.
- [2] Czubyko U, Sursaeva VG, Gottstein G, Shvindlerman LS. Acta Mater 1998;46:5863.
- [3] Gottstein G, Shvindlerman LS. Acta Mater 2002;50:703.
- [4] Gottstein G, Ma Y, Shvindlerman LS. Acta Mater 2005;53:1535.
- [5] Mattissen D, Molodov DA, Shvindlerman LS, Gottstein G. Acta Mater 2005;53:2049.
- [6] Protasova SG, Gottstein G, Molodov DA, Sursaeva VG, Shvindlerman LS. Acta Mater 2001;49:2519.
- [7] Hsieh TE, Balluffi RW. Acta Metall 1989;37:2133.
- [8] Watson GM, Gibbs D, Song S, Sandy AR, Mochril SGJ, Zener DM. Phys Rev 1995;52:12329.
- [9] Lee SB, Yoon DY, Henry MB. Acta Mater 2000;48:3071.
- [10] Rabkin E. J Mater Sci 2005;40:875.
- [11] Sursaeva VG, Straumal BB, Gornakova AS, Shvindlerman LS, Gottstein G. Acta Mater 2008;56:2728.
- [12] Gottstein G, Shvindlerman LS, Sursaeva VG. Int J Mater Res 2008;52:491.
- [13] Barrales-Mora LA, Shvindlerman LS, Mohles V, Gottstein G. Mater Sci Forum 2007;558:1051.
- [14] Barrales-Mora LA, Shvindlerman LS, Mohles V, Gottstein G. Acta Mater 2008;56:1151.
- [15] Barrales-Mora LA, Gottstein G, Shvindlerman LS. Acta Mater 2008;56:5915.

- [16] Gottstein G, Murmann HC, Renner G, Simpson C, Lücke K. In: Gottstein G, Lücke K, editors. *Textures of materials*. Berlin: Springer-Verlag; 1978. p. 521.
- [17] Koo JB, Yoon DY. *Metall Mater Trans A* 2001;32:469.
- [18] Kirch DM, Zhao B, Molodov DA, Gottstein G. *Scripta Mater* 2007;56:939.
- [19] Kazaryan A, Wang Y, Dregia SA, Patton BR. *Acta Mater* 2002;50:2491.
- [20] Straumal BB, Rabkin E, Sursaeva VG, Gornakova AS. *Z Metallkd* 2005;96:96.
- [21] Herring C. *Phys Rev* 1951;82:87.
- [22] Cahn JW, Hoffman DW. *Acta Metall* 1974;22:1205.
- [23] Davidson D, den Nijs M. *Phys Rev E* 2000;59:5029; *Phys Rev Lett* 2000;84:326.
- [24] Rottman C, Wortis M. *Phys Rep* 1984;103:59.
- [25] Heyraud JC, Métois JJ. *J Cryst Growth* 1987;82:269.
- [26] Straumal BB, Sursaeva VG, Baretzky B. *Scripta Mater* 2010;62:924.
- [27] Schulz LG. *J Metals* 1954;6:1082.
- [28] Aristov VV, Shulakov EV. *J Appl Crystallogr* 1975;8:445.
- [29] Antonov AV, Kopetskii ChV, Shvindlerman LS, Sursaeva VG. *Sov Phys Dokl* 1974;18:736.
- [30] Antonov AV, Kopetskii ChV, Shvindlerman LS, Sursaeva VG. *Institute of Solid State Physics, Chernogolovka*; 1972.